2014 IEEE International Conference on Robotics & Automation (ICRA)
Hong Kong Convention and Exhibition Center
May 31 - June 7, 2014. Hong Kong, China

Harmonic PZT Poly-Actuators

James Torres, Lluis Penalver-Aguila, and H. Harry Asada, *Member, IEEE*

***Abstract*— Capacitive actuators, such as piezoelectric stack actuators, provide an efficient solution for robotic and mechatronic systems that typically require large forces and minimal velocities over long periods of time. To overcome the stack actuator's limitations, particularly their limited stroke, a harmonic poly-actuator design is presented. This design utilizes a multitude of intermediate buckling amplification mechanisms in a parallel arrangement to create a large stroke, high force actuator. The redundant system architecture combined with a particular spatial and temporal coordination allow for a number of salient features, including robustness to failure, backdrivability, and continuous force control via elementary ON-OFF control. A prototype was built using six intermediate buckling amplification mechanisms and was able to produce over 100 Newtons of force over a stroke of 450 mm.**

I. Introduction

Piezoelectric stack actuators, such as lead-zirconate-titanate (PZT), have several desirable properties for robotic and mechatronic systems including: a high bandwidth above 100 kHz, power density over 10^8 $^{W}/_{m^3}$, and efficiencies greater than 90% [1]. Furthermore, PZT stacks have two other major benefits: first, they are capacitive actuators and therefore, are highly efficient in maintaining large forces at a constant position. Second, they are backdrivable, which can be essential for safe robotic systems. The major practical limitation is their limited strain, typically around 0.1%, that prevent PZT stacks from directly driving robotic systems.

In order to compensate for the limited stroke of the PZT stack, mechanical amplification devices have been developed to greatly increase the effective displacement. Most of these devices rely on aligning the PZT stacks at a shallow angle with respect to each other and connecting them via rotational joints comprised of flexures. Typically their displacement amplification gain is 10 or less [2][3]. In order to achieve larger amplification, these designs can be arranged in a nested architecture [4]. This paper will focus on a unit that is able to produce amplification gain of 100 or greater within a single stage, as discussed in detail here [5].

For a system requiring position control via feedback, these amplified mechanisms can be sufficient, but at most only produce displacements an order of magnitude less than their length scale. In contrast, linear actuators, such as solenoids to hydraulics, produce a stroke on the order of the length scale of the actuator itself. Furthermore, regardless of the amplification mechanism, PZT actuators in general produce a force output that is a function of the displacement, which individually limits its force control capabilities.

Long-stroke linear or infinite stroke rotary piezoelectric actuators have been developed. The most prevalent type are ultrasonic motors (USM). These motors utilize a cyclic, high frequency input to produce continuous motion. However, due to their reliance on friction, their power density is significantly lowered, around 10^4 $^{W}/_{m^3}$ [2]. The lack of effective means to match impedance between the PZT stack and the load is another factor for the low power density.

Beyond USM, there are many ways of converting cyclic motion into continuous output. This paper considers a design where cyclic motion is produce by the amplification unit as opposed to the piezoelectric actuator directly. Due to the larger displacement and proportionally lower force, it becomes mechanically feasible to convert the unit's cyclic motion into a long-stroke displacement output by acting on a sloped surface similar to a gear, instead of relying on friction. This can be more efficient than USM and the particular geometry of the surface provides the ability to effectively interface the output mechanism to the load.

The mechanism described above can be extended to one in which multiple PZT units are engaged with the output gear teeth so that a larger force can be generated collectively by the arrayed PZT units. We refer to this arrangement as a poly-actuator. Generally, a poly-actuator combines several simple units in series, parallel or both. Poly-actuators provide several salient features over a single actuator, including simplified individual control, for example ON-OFF control can often times be sufficient, reduction of hysteresis [6], and robustness to failures [7].

This paper will discuss the design concept of a particular poly-actuator using the amplified PZT units arranged along the output rod. See Fig. 1. Note that the PZT units comprise of amplification mechanisms that produce a displacement large enough to transverse the depth of the gear teeth [5][8]. Analysis of the force characteristics with regard to position and input voltage are discussed. A simplified ON-OFF controller is considered. The initial implementation of a functional prototype is shown along with experimental results of the output force properties.

II. Design Concept of Harmonic PZT Poly-Actuators

The harmonic PZT poly-actuator relies on several identical amplification units all acting in parallel on a single output. Figure 2 shows the schematic of a buckling displacement amplification mechanism [5][8] used for the poly-actuator.

J. Torres and L. Penalver-Aguila are with the Department of Mechanical Engineering, Massachusetts Institute of Technology, 77 Massachusetts Ave., Cambridge, MA 02139 USA (phone: 617-258-0811; email: jtorres9@mit.edu)

H. Asada is with the Faculty of Mechanical Engineering, Massachusetts Institute of Technology, 77 Massachusetts Ave., Cambridge, MA 02139 USA (email: asada@mit.edu)

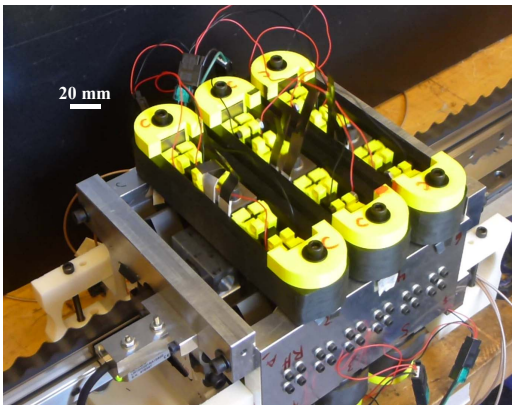

Fig. 1. A picture of an harmonic piezoelectric poly-actuator prototype. Note the size of the gear teeth that allows the unit's cyclic motion to be converted into a long-stroke displacement output without relying on friction.

When a voltage is applied to the PZT stacks, they expand, with displacement z, from the initial kinematically singular position in the center and rotate by angle θ about the grounded rotational joints creating a vertical displacement, y, at the output node. This mechanism is able to produce a displacement amplification of two orders of magnitude within a single stage due to the immense instantaneous gain near the kinematic singularity as well as the ability to displace both upwards and downwards in bi-polar motion.

This buckling amplification mechanism becomes the basic unit within the poly-actuator, shown in Fig. 3. The vertical arrows demonstrate the displacement direction of the individual units, whereas the horizontal arrow shows the direction of the poly-actuator output. These units are equally spread along one-half of the wavelength of the output waveform. Note that they are spread over one-half the wavelength due to the symmetric bi-polar stroke of the buckling unit. For a given input, there is no difference with regards to the poly-actuator output between the first and second half of the waveform. The amplitude, A, of the waveform is equal to the free displacement of the buckling unit in the vertical direction, y. For this particular poly-actuator, the waveform is a sinusoid, with a spatial frequency, ω, that is proportional to the poly-actuator output velocity and inversely proportional to the poly-actuator output force. The location of the individual units is indicated by the gear phase, φ, which relates directly to the gear position, X, as shown in the figure.

The objective of this paper is to exploit salient features of poly-actuators consisting of multiple PZT units. A critical condition for exploiting these features is the equal spacing of the units along the half wavelength. This provides two important features: first, it ensures there is never a point where all of the units are in a kinematically singular configuration, and second, it balances each of the units to regulate the total force generated by the multiple PZT units despite the displacement-dependent output force of individual units and their pronounced nonlinearity.

Within one full wavelength of the gear there are four points where each unit is in a kinematic singularity, the two peaks and the two center points. The peaks are a kinematic singularity because the slope of the gear is zero and therefore, the buckling unit cannot impose a force on the output. The center points are kinematic singularities because the buckling mechanism is in its kinematic singular configuration, as shown in Fig. 2, where the unit cannot impose a force on the output node. If the units are equally spread along a half wavelength, the maximum number of units that can be at a kinematic singularity is two, regardless of the total number of units. As will be proven later, this then imposes a constraint that the minimum number of actuators to ensure the poly-actuator itself is never in a kinematic singularity is three.

As mentioned earlier, the stroke of the amplification mechanism is limited to the inherent stiffness of the PZT stack. We will show that through the proper placement of the buckling units the adverse effect of the PZT stack stiffness disappears and the output force becomes solely reliant on the input command and the gear phase, φ. Similarly, this is proven in the next section.

Both of these properties are directly related to the sinusoidal waveform of the gear, and therefore yield the name "harmonic" PZT poly-actuator.

III. Kinematic and Static Analysis

The individual units within the linear poly-actuator have significantly non-linear force-displacement relationships that are further transformed by the shape of the gear. Each unit

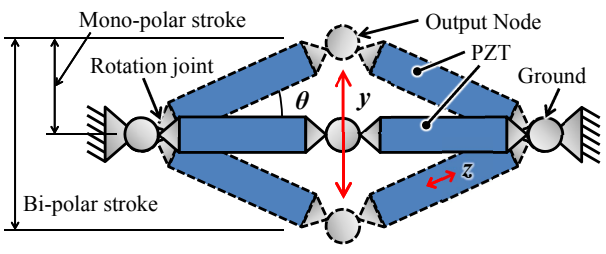

Fig. 2. A simple diagram of the buckling amplification mechanism, demonstrating the bi-polar stroke. As the PZT stacks are energized, the output node deviates from the kinematic singularity in the center and "buckles" upwards or downwards.

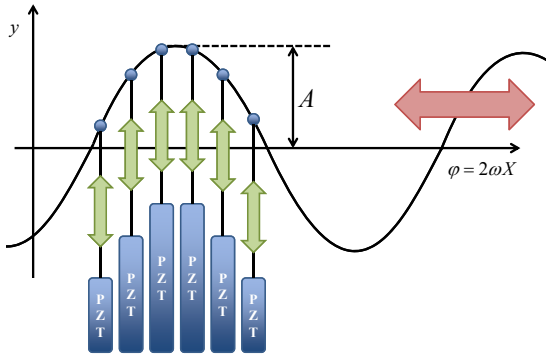

Fig. 3. This schematic demonstrates several general PZT units acting in parallel on a single poly-actuator output shaft. The amplitude, A, is tuned to match the free displacement of the PZT units, whereas the spatial frequency, ω, defines the speed-force relationship.

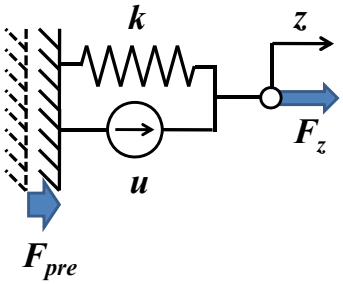

Fig. 4. A lumped parameter model of the a PZT stack, including a preload force, f_{pre}, input, u, and spring with stiffness k.

can be controlled via a variety of algorithms to achieve multiple salient properties in the poly-actuator, however, in this paper we will only explore ON-OFF control. The resultant output force of the poly-actuator depends on:

a) the force-displacement characteristics of each PZT stack,
b) the buckling amplification mechanism geometry,
c) the shape of the output shaft, and
d) the number and spatial distribution of the PZT units.

a) We consider a simple spring-force source model for the PZT stack, shown in Fig. 4:

$$f_z = u - kz + f_{pre} \tag{1}$$

where f_z is the output force, k is the mechanical stiffness, and z is the displacement of the PZT stack. We assume that the applied voltage is proportional to the net force u, which is attenuated due to the PZT stack stiffness, k and added by the preload, f_{pre}.

b) Figure 5 shows the buckling displacement amplification mechanism, and from the figure it is evident that each PZT stack generates a force $f_z \sin\theta$ in the y-direction. Also acting on the output node is a restoring force generated by the preload compensation spring (PCS), which is to apply a constant force to the PZT, i.e. a preload [5]. Adding these forces, each buckling unit produces the y-directional force given by:

$$f_y = -k_y y + 2 f_z \sin\theta \tag{2}$$

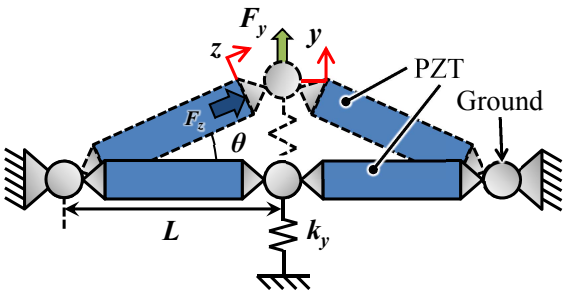

Fig. 5. The upward force, f_y, becomes larger as the PZT stacks rotate by angle θ, however, this is counteracted by the decrease in PZT force due to the elongation of the PZT stack, z.

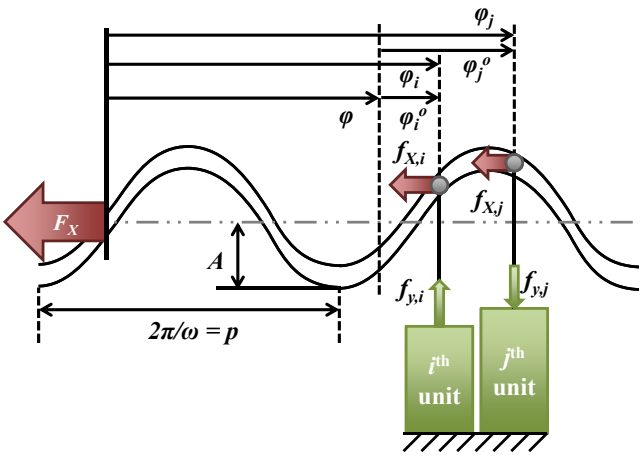

Fig. 6. The output force from each unit is transmitted through the gear, and even if individual units are acting in opposite directions, due to the change in the slope of the gear they can still contribute a force in the same direction.

Using approximate relationships, $\sin\theta \approx \frac{y}{L}$ and $z \approx \frac{y^2}{2L}$ and setting $f_{pre} \equiv \frac{k_y L}{2}$, we attain:

$$f_y = \frac{2u}{L} y - \frac{k}{L^2} y^3 \tag{3}$$

c) The buckling amplification unit interfaces directly with a sinusoidal output shaft, as shown in Fig. 6, with amplitude A, pitch p, and linear position X. The pitch, p, can is related to the spatial frequency, ω; $\omega = \frac{2\pi}{p}$. The position X can be converted to a phase angle φ; $\varphi = 2\omega X$. The output force of the buckling mechanism, f_y, is transformed by the instantaneous slope at the contact point, $\frac{dy}{dX}$. The unit displacement, y, is a function of gear position, X, and therefore, the overall output force of the unit is described in Eqs. 4-7.

$$f_X = f_y \cdot \frac{dy}{dX} \tag{4}$$

The buckling unit displacement, y, is related to the gear position, X, through a sinusoidal relationship: $y = A \sin\omega X$. Therefore, Eq. 4 can be expressed with respect to the input, u, and the gear position, X.

$$f_X = \left\{ \frac{2u}{L} A \sin\omega X - \frac{k}{L^2} [A \sin\omega X]^3 \right\} \left(\frac{2\pi A}{p} \cos\omega X \right) \tag{5}$$

Using several trigonometric identities, Eq. 5 can be simplified into:

$$f_X = C \left[(u - f_o) \sin(\varphi) + \frac{1}{2} f_o \sin(2\varphi) \right] \tag{6}$$

where:

$$C \triangleq \frac{2\pi A^2}{pL}, f_o \triangleq \frac{kA^2}{4L} \tag{7}$$

$$F_X = \sum_{i=1}^{n} f_{X,i};\; f_{X,i} = C\left\{(u_i - f_o)\sin\varphi_i + \tfrac{1}{2} f_o \sin(2\varphi_i)\right\};\; u_i = u_i(\varphi_i);\; \varphi_i = \varphi + \varphi_i^o, \varphi_{\mathrm{i}}^{\mathrm{o}} = 2\pi\tfrac{\mathrm{i}}{\mathrm{n}}, \mathrm{i} = 1\ldots\mathrm{n}$$
$$F_X = C\sum_{i=1}^{n} u_i \sin\varphi_i - Cf_o\sum_{i=1}^{n}\sin\varphi_i + \tfrac{1}{2}Cf_o\sum_{i=1}^{n}\sin(2\varphi_i) \tag{8}$$

$$F_X = C\sum_{i=1}^{n} u_i \sin\varphi_i - Cf_o\left[\sin\varphi\sum_{i=1}^{n}\cos\varphi_i^o + \cos\varphi\sum_{i=1}^{n}\sin\varphi_i^o + \frac{1}{2}\sin 2\varphi\sum_{i=1}^{n}\cos 2\varphi_i^o + \frac{1}{2}\cos 2\varphi\sum_{i=1}^{n}\sin 2\varphi_i^o\right] \tag{9}$$

Note C is a dimensionless gain associated with the geometry of the amplification unit and output gear. Furthermore, if A is equal to the free displacement of the buckling actuator, the force, f_o, is to half the blocking force of the PZT which essentially provides a bias that ensures the output force is bidirectional.

d) The above expression only represents the gear output force from a single buckling unit. The poly-actuator has several units acting simultaneously. Furthermore, as mentioned previously, they are evenly distributed over one-half wavelength. The relative phase position, φ_i^o a constant, is defined below. The total poly-actuator output force, shown in Eq. 8, can be expressed as a summation of each of the contributions form the individual units, where the subscript i denotes the i-th unit out of n total units. Separating the global gear position φ from the individual unit positions φ_i yields Eq. 9.

Note that the last four summations are all constants determined by the distribution of the units. The interaction between multiple units leads to the cancellation of every term except those directly affected by the control efforts, u_i, provided the number and distribution of actuators is properly balanced. The four constant summations are identically zero if φ_i^o is defined as above in Eq. 8 and $n > 2$. A proof of this phenomenon can be found in Appendix I. Therefore, the final expression for the poly-actuator output force is:

$$F_X = C\sum_{i=1}^{n} u_i \sin\varphi_i, n > 2 \tag{10}$$

IV. Output Force Control

For the purposes of this paper, we will consider solely ON-OFF control, i.e. inputs of $u_i = 0$ or $u_i = 1$. For a large number of PZT units, $n \gg 1$, the simple ON-OFF controls can generate an output force that varies almost continuously. For a smaller number of units, the output force resolution is inevitably limited. However, this analysis can still provide insight into its general functionality. Furthermore, this method of powering the PZT stacks is more efficient as providing a continuous voltage via a linear amplifier consumes a significant amount of power regardless of the loading condition. Previous research has improved efficiencies even further by utilizing capacitors [9] or other PZT stacks [10] to store electrical energy not transmitted to the mechanical load.

A. Backdrivability

The ability to drive the actuator from the output, "backdrivability", can be a particularly desirable property for robotic applications. Consider the situation where all of the buckling units are held at the same input force, $\hat{u}$. The total gear output force becomes:

$$F_X = C\sum_{i=1}^{n} \hat{u}\sin\varphi_i = 0 \tag{11}$$

Similar to the case in Eq. 10, the summation is identically equal to zero if the inputs are identical. Therefore, the output force is equal to zero for all positions. It is more efficient to hold all of the inputs at zero as opposed to a non-zero value to prevent power from being wasted if the gear is moved. This is one example where, due to redundancy, there are multiple inputs that provide the same poly-actuator output force, but clearly there are significant advantages when considering metrics beyond solely the output force.

B. Average Output Force Control

To achieve a non-zero output force while constrained to only ON-OFF control of the individual units, there are two control variables: the charging phase, φ_c, and the discharging phase, φ_d, shown in Fig. 7. In this situation, each unit determines its individual phase, φ_i and is held ON or OFF based on its position relative to the charging and discharging phases.

Unlike the backdrivable case, the instantaneous poly-actuator output force, F_X, varies with the phase position, φ.

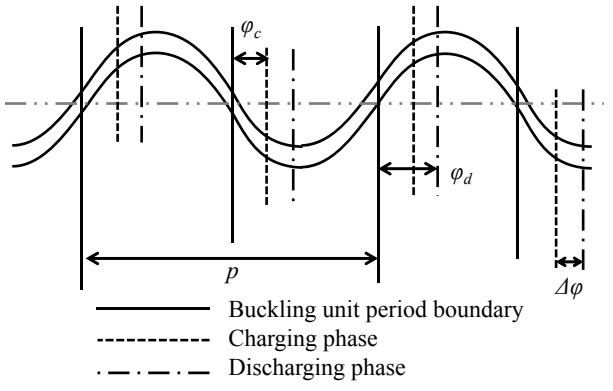

Fig. 7. A schematic of sample locations of the charge and discharge phase. Any unit within the band, $\Delta\varphi$, will be turned ON, otherwise the unit is OFF.

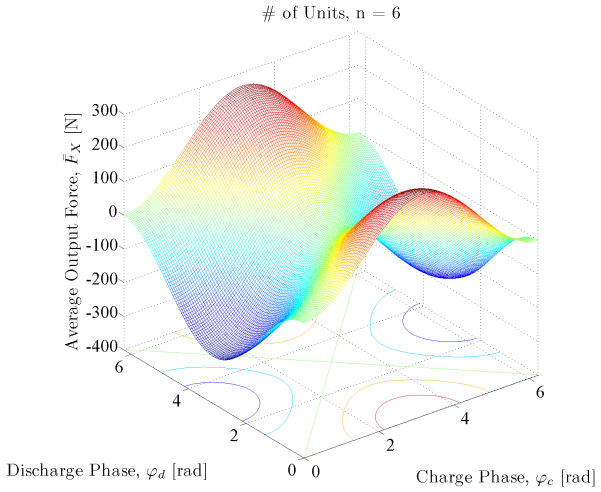

Fig. 8. A smooth surface showing the average poly-actuator output force as a function of both the charge and discharge phase. Note the plot is symmetric as the actuator has no preferred direction. Furthermore, the contours on the φ_c-φ_d plane show lines of constant average output force.

However, the average poly-actuator output force, $\bar{F}_X$, can be evaluated by integrating the force over one cycle and dividing by 2π, as shown below, where $u_{\max}$ is the ON input condition.

$$\begin{aligned}\bar{F}_X &= \sum_{i=1}^{n} \frac{1}{2\pi} \int_0^{2\pi} f_{X,i} d\varphi_i = \frac{n}{2\pi} \int_0^{2\pi} Cu(\varphi) \sin\varphi d\varphi \\ &= \frac{nCu_{\max}}{2\pi} \left[\cos\varphi_c - \cos\varphi_d\right]\end{aligned} \tag{12}$$

With the two independent inputs, φ_c and φ_d, a continuous range of average poly-actuator output forces, $\bar{F}_X$, is possible. As Fig. 8 shows, with the exception of the peak force, there are contours within the φ_c-φ_d plane that produce a constant average output force due to the redundancy in the system. Along these contours, the particular force profile can vary significantly and deciding which particular control input is determined by other desired characteristics, such as the RMS value of the force deviation, the peak or minimum force, or the total phase charged.

A closed form solution for the force ripple, F_{rms}, cannot be explicitly solved for but it can be defined as the RMS deviation from the average force, $\bar{F}_X$:

$$F_{rms} \triangleq \sqrt{\frac{1}{2\pi} \int_0^{2\pi} \left[F_X(\varphi) - \bar{F}_X\right]^2 d\varphi} \tag{13}$$

V. Prototype Implementation and Experimental Results

For the initial prototype, shown in Fig. 9, six buckling units were connected to an output gear with a stroke of 450 mm. Table I summarizes the design parameters and the expected performance of the individual units and the overall poly-actuator.

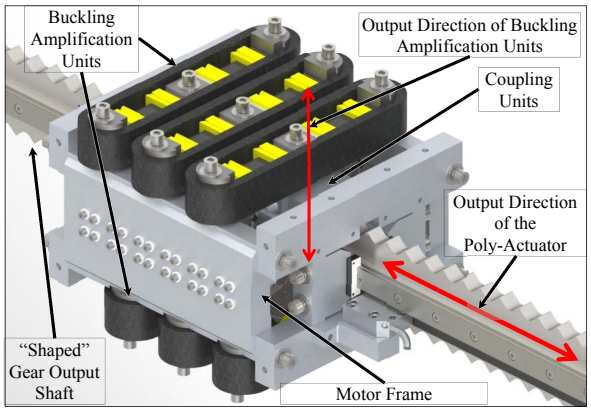

Fig. 9. A labeled 3D rendering of the harmonic PZT poly-actuator prototype.

TABLE I
Summary of Parameters of the Alpha Prototype

Constant / Variable	Symbol	Value / Range
PZT input force	u	0-3675 N
PZT displacement	z	0-42 μ m
PZT stiffness	k	8.75 $\times 10^7$ N/m
PZT output force	f_z	$\pm$ 3675 N
PZT preload force	f_{pre}	5000 N
Buckling mechanism displacement	y	$\pm$ 2.5 mm
Buckling mechanism output force	f_y	$\pm$ 230 N
Buckling mechanism	L	75 mm
PCS stiffness	k_y	1.3 $\times 10^5$ N/m
Gear displacement	X	0-450 mm
Gear pitch	p	15 mm
Gear amplitude	A	2.5 mm
Poly-actuator output force	F_X	$\pm$ 260 N
Number of buckling units	n	6

The buckling units were constrained using carbon fiber reinforced plastic to save weight while maintaining a high stiffness which is necessary to transmit a large percentage of the energy through the PZT stacks. [5] However, the frames had a measurable variation in stiffness due to manufacturing defects that caused a significant degradation in the overall performance of the poly-actuator.

A comparison was made between the model and the measured force-gear phase relationship (F_X versus φ) for the maximum poly-actuator output force control, i.e. $\varphi_c = 0$ and $\varphi_d = \pi$, shown in Fig. 10.

There is a large discrepancy, approximately a factor of 2, difference between the model and the measurement. This is largely due to the fact that the force output characteristics of the poly-actuator rely heavily on having the individual units balanced. This requires three major parameters to be accurate: a) the relative phase position, φ_i^o, b) the preload force, f_{pre}, and c) the stiffness of the PZT stack, k. Based on machining tolerances and measurements of the individual units, respectively, we confirmed that the first two parameters were accurate to within 5%. However, the modeled stiffness of the PZT stack varied significantly from unit to unit by over

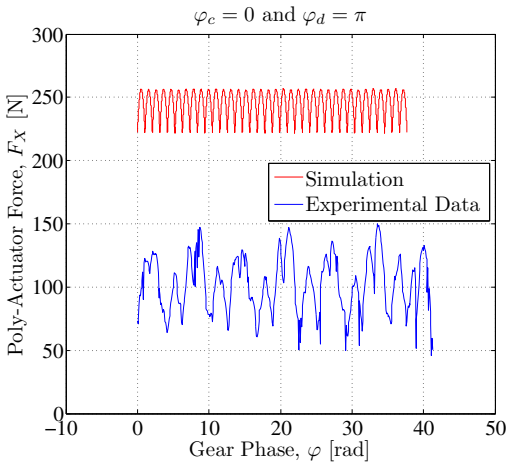

Fig. 10. The plot shows the modeled and experimental force output for charging phase of $\varphi_c = 0$ and a discharging phase of $\varphi_d = \pi$. The large discrepancy likely is due to significant variation in the preload force, f_{pre} and the effective PZT stiffness, k.

20%. The physical stiffness of the individual PZT stacks have a much higher manufacturing repeatability, but the initial model in Fig. 4 is a lumped parameter model whose stiffness takes into account the frame and crucial components of the buckling mechanism.

The unbalanced units prevented the pure backdrivability as well. Instead of having no output force for all positions and a constant input, the force ripple was approximately 20 N, just under 10% of the theoretical maximum poly-actuator output force. The performance was consistent, however, with Eq. 9, when considering unbalanced parameters.

VI. Conclusions

A harmonic PZT poly-actuator was shown to collectively use the redundant PZT units with a specific spatial distribution of units along the output shaft to produce a continuous range of average output forces over a large-stroke. The proper placement of the, ideally, identical individual units allows for them to balance their inherent stiffness to provide an output force that relies solely on the input. This allowed for the poly-actuator to be backdrivable, i.e. zero output force for all positions, if all of the inputs are equal. Furthermore, the redundancy allowed for a set of inputs to impose the same average poly-actuator output force. Therefore, additional metrics, such as force ripple, peak force, or total time the units are ON, could be considered as well. In implementation, however, the units varied significantly enough that the measured output was approximately half of the modeled poly-actuator output force. Providing more consistent, repeatable units will improve the output characteristics. Furthermore, expanding the control algorithms beyond ON-OFF will allow for possible compensation of the discrepancies between units.

Appendix

A. Proof of Balancing Units

The spacing of the units is defined in Eq. 8; $\varphi_i^o \triangleq 2\pi\frac{i}{n}$. Therefore, considering the summations in the second and third terms in Eq. 9:

$$\sum_{i=0}^{n-1} \cos\left(\varphi_i^o\right) + j\sum_{i=0}^{n-1} \sin\left(\varphi_i^o\right) = \sum_{i=0}^{n-1} \left(e^{\frac{2\pi j}{n}}\right)^i \tag{14}$$

If the quantity in Eq. 14 is shown to be zero, then both summations must be zero. This quantity can be simplified by using the following identity associated with the summation of a geometric series:

$$\sum_{i=0}^{n-1} r^i = \frac{1-r^n}{1-r}, \text{ if } r \neq 1 \tag{15}$$

Therefore, Eq. 14 can be simplified to:

$$\sum_{i=0}^{n-1} \left(e^{\frac{4\pi j}{n}}\right)^i = \frac{1-\left(e^{\frac{2\pi j}{n}}\right)^n}{1-e^{\frac{2\pi j}{n}}} = \frac{1-1}{1-e^{\frac{2\pi j}{n}}} = 0 \tag{16}$$
$$r = e^{\frac{2\pi j}{n}} \neq 1 \Rightarrow n > 1$$

Similarly, the fourth and fifth terms in Eq. 9 are equal to zero:

$$\sum_{i=0}^{n-1} \left(e^{\frac{4\pi j}{n}}\right)^i = \frac{1-\left(e^{\frac{4\pi j}{n}}\right)^n}{1-e^{\frac{4\pi j}{n}}} = \frac{1-1}{1-e^{\frac{4\pi j}{n}}} = 0 \tag{17}$$
$$r = e^{\frac{4\pi j}{n}} \neq 1 \Rightarrow n > 2$$

References

[1] J. Huber, N. Fleck, and F. Ashby, "The selection of mechanical actuators based on performance indices," *Mathematical, Physical and Engineering Sciences*, vol. 453, no. 1965, pp. 2185–2205, 1997.

[2] C. Niezrecki, D. Brei, S. Balakrishnan, and A. Moskalik, "Piezoelectric actuation: State of the art," *The Shock and Vibration Digest*, vol. 33, no. 4, pp. 269–280, 2001.

[3] E. Furukawa, M. Mizuno, and T. Doi, "Development of a flexure-hinged translation mechanism driven by two piezoelectric stacks," *JSME International Journal*, vol. 38, no. 4, pp. 743–748, 1995.

[4] T. Secord and H. Asada, "A variable stiffness PZT actuator having tunable resonant frequencies," *IEEE Transactions on Robotics*, vol. 26, no. 6, pp. 993–1005, 2010.

[5] J. Torres and H. Asada, "High-gain, high transmissibility PZT displacement amplification using a rolling-contact buckling mechanism and preload compenstions springs," *IEEE Transactions on Robotics*, 2014. Manuscript submitted for publication.

[6] L. O. J. Ueda and H. Asada, "Broadcast feedback of stochastic cellular actuators inspired by biological muscle control," *International Journal of Robotics Research*, vol. 26, no. 11, pp. 1251–1265, 2007.

[7] A. Girard and J.-S. Plante, "Applied control of binary robots based on inuence vectors," in *Proceedings of the IEEE International Conference on Robotics and Automation*, pp. 523–529, May 2013.

[8] D. Neal and H. Asada, "Bipolar piezoelectric buckling actuators," *IEEE/ASME Transactions on Mechatronics*, vol. 19, pp. 9–19, February 2014.

[9] D. Campolo, M. Sitti, and R. Fearing, "Efficient charge recovery method for driving piezoelectric actuators with quasi-square waves," *IEEE Transactions on Ultrasonics, Ferroelectrics and Frequency Control*, vol. 50, no. 3, pp. 237–244, 2003.

[10] P. Barragan and H. Asada, "Design of energy-saving PZT drive amplifiers for mobile and wearable physical assists," in *Proceedings of the ASME 2011 Dynamics Systems and Control Conference*, pp. 783–790, October 2011.